

Fast converging path integrals for time-dependent potentials: I. Recursive calculation of short-time expansion of the propagator

Antun Balaž^{1,2}, Ivana Vidanović¹, Aleksandar Bogojević¹, Aleksandar Belić¹ and Axel Pelster³

¹ Scientific Computing Laboratory, Institute of Physics Belgrade, University of Belgrade, Pregrevica 118, 11080 Belgrade, Serbia⁴

² Department of Physics, Faculty of Sciences, University of Novi Sad, Trg Dositeja Obradovića 4, 21000 Novi Sad, Serbia

³ Fachbereich Physik, Universität Duisburg-Essen, Lotharstraße 1, 47048 Duisburg, Germany

E-mail: antun@ipb.ac.rs, ivanavi@ipb.ac.rs, alex@ipb.ac.rs, abelic@ipb.ac.rs and axel.pelster@uni-duisburg-essen.de

Received 5 December 2010

Accepted 6 February 2011

Published 4 March 2011

Online at stacks.iop.org/JSTAT/2011/P03004

[doi:10.1088/1742-5468/2011/03/P03004](https://doi.org/10.1088/1742-5468/2011/03/P03004)

Abstract. In this and the subsequent paper (Balaž *et al* 2011 *J. Stat. Mech.* P03005) we develop a recursive approach for calculating the short-time expansion of the propagator for a general quantum system in a time-dependent potential to orders that have not been accessible before. To this end the propagator is expressed in terms of a discretized effective potential, for which we derive and analytically solve a set of efficient recursion relations. Such a discretized effective potential can be used to substantially speed up numerical Monte Carlo simulations for path integrals, or to set up various analytic approximation techniques to study properties of quantum systems in time-dependent potentials. The analytically derived results are numerically verified by treating several simple models.

Keywords: other numerical approaches, quantum Monte Carlo simulations, series expansions, diffusion

⁴ <http://www.scl.rs/>.

Contents

1. Introduction	2
2. Path-integral formalism for systems with time-dependent potentials	4
3. Path-integral calculation of the propagator	7
4. Forward and backward Schrödinger equation	11
5. Recursive calculation of the propagator for one-dimensional systems	13
6. Numerical verification	16
7. Conclusions	21
Acknowledgments	21
References	22

1. Introduction

Studying quantum systems in time-dependent potentials represents a fundamental problem which emerges in many areas of physics. Even if the Hamiltonian of the system itself does not explicitly depend on time, such situations naturally occur in the presence of time-dependent external fields. Another important example are fast-rotating systems, where the rotation introduces an explicit time dependence of the respective variables in the co-rotating frame. This includes modern experiments with rotating ultracold atoms and Bose–Einstein condensates [2]–[9], studies of vortices [10, 11], and non-stationary optical lattices [12]–[14]. In the latter case counter-propagating laser beams are not perfectly modulated, so they produce an effectively moving optical lattice. An explicit treatment of time-dependent problems is also often required in nuclear and molecular physics [15], and in studies of entanglement phenomena [16]–[18]. Note that some systems can also be treated effectively with a time-dependent potential, which actually represents higher nonlinear terms in the wavefunction. A prominent example is the Gross–Pitaevskii equation, where the nonlinear term is treated within the split-step Crank–Nicolson method as a time-dependent potential which is updated after each time step [19].

A time-dependent formalism has been developed in the framework of various theoretical approaches, based on the time-dependent Schrödinger equation. The well-known time-dependent semiclassical approximation is formulated by the Van Vleck propagator, and provides a wide range of important results, including generalizations to the time-dependent variational perturbation theory. The time-dependent variational principle, formulated by Dirac, forms the basis for the time-dependent self-consistent fields method [20]. Another general method is time-dependent perturbation theory, which is also applied to derive a number of other approaches, including time-dependent scattering theory, linear response theory (Kubo formula) and Fermi’s golden rule. Path-integral formalism [21] also provides a general framework to study the dynamics of time-dependent quantum systems. In addition to these general methods, time-dependent variants of

many highly specialized methods have also been developed. As important examples, let us mention the time-dependent density matrix renormalization group (DMRG) [22, 23], the density functional theory (DFT) [24, 25], and the density matrix functional theory (DMFT) [26].

In numerical approaches for time-dependent systems, a partial differential equation representation of the time-dependent Schrödinger equation can be solved using the discretization of the time domain through the finite difference method. In this case, the specific techniques include both explicit and implicit schemes, for example the commonly used Crank–Nicolson scheme [27]. Other major numerical approaches include molecular dynamics, as well as the split operator method, which is based on a space-grid calculation both without [28, 29] and with Monte Carlo [30, 31] techniques. This method is mainly used in its second-order variant in the time of propagation for time-dependent potentials, where no change is required in comparison with the time-independent case. However, also higher-order split operator schemes have been derived, including fourth [32]–[35] and higher-order expansions [36]–[39]. We also mention important counterexamples, such as world-line Monte Carlo [40]–[42], where discretization errors are completely removed [43], or open systems where the main contribution to the systematic error is due to retardation effects which cannot be dressed into the form of simple potentials [44].

In this and the subsequent paper [1], we extend the earlier established approach in [45]–[48] for obtaining a high-order short-time expansion of transition amplitudes of time-independent potentials to the important time-dependent case. This development allows a high-precision calculation of transition amplitudes, which is necessary for extracting the properties of various quantum systems, such as partition functions. Note that individual transition amplitudes can be accurately calculated using the lower-order effective actions at the expense of increasing the number of Monte Carlo time steps, which would just increase the required computation time. Although the presented approach can be used to improve the efficiency of calculating such transition amplitudes, it is mainly developed for applications which require a large number of accurate transition amplitudes for further numerical calculations. Such situations occur, for instance, when determining partition functions [47, 49] or for obtaining energy spectra with the method of diagonalizing the space-discretized evolution operator matrix [50, 51]. In order to avoid an accumulation of numerical errors, so that such calculations can be performed with the required accuracy, the transition amplitudes have to be known more precisely.

Our approach has already been successively used to study global and local properties of rotating Bose–Einstein condensates [52], where the availability of accurately calculated thermal states has allowed the precise calculation of the condensation temperature, the ground-state occupancy, and time-of-flight absorption pictures even in the delicate regime of a critical and an overcritical rotation. If one needs large numbers of accurate energy eigenvalues and eigenstates, as in this case, higher-order effective actions become useful. The precise knowledge of the short-time expansion of the propagator might also be used to improve numerical studies of time evolution, especially in systems exhibiting nonlinearities [28], where a time-dependent formalism is required. In addition to this, the presented approach can offer a significant improvement in studying dynamics of quantum systems within the path-integral Monte Carlo calculations. The multilevel blocking method [53] might be used to address the inherent dynamical sign problem, while the

required number of Trotter time slices may be significantly decreased, due to high order of convergence of short-time propagators derived here.

Thus, in spirit of Symanzik's improved action program in quantum field theory [54, 55], we will introduce and analytically derive effective actions for time-dependent potentials which substantially speed up the numerical calculation of transition amplitudes and other quantities for such quantum systems. This approach does not suffer from the technical problems related to backwards diffusion in time, as observed and discussed by Sheng [56] and Suzuki [57]. In the split operator method one has to resort to multi-product expansions [58] in order to resolve this problem. In the higher-order effective action approach for time-dependent potentials, which is presented here, the convergence of transition amplitudes is always guaranteed in a natural way, as was shown conclusively for the time-independent case in [59]. While this approach has a number of benefits (systematic higher-order expansion, simple implementation of symbolic calculation of effective actions using recursive relations, unconditional convergence of transition amplitudes in the imaginary-time formalism, simple numerical implementation of the algorithm), it also has some disadvantages when compared to other short-time approaches. Most notably, higher-order effective action in this method contain higher spatial and time derivatives of the potential, and thus require the potential to be a smooth function. Another possible disadvantage is the increasing computational complexity of higher-order effective actions, which significantly grows with the order, and has to be appropriately chosen so as to minimize the computing time for the desired precision of numerical calculations.

The outline of this paper is as follows. In section 2 we briefly review the underlying path-integral formalism of quantum mechanics [21], [60]–[62] for systems in time-dependent potentials in order to fix our notation. Afterward, section 3 presents a lowest-order path-integral calculation of the short-time transition amplitude for time-dependent potentials in the single-particle one-dimensional case. Based on these lowest-order results and using Schrödinger equations for transition amplitudes of systems in time-dependent potentials derived in section 4, we develop in section 5 the systematic efficient recursive approach for one-dimensional quantum systems. The analytically derived results are verified numerically with the help of several illustrative one-dimensional models in section 6.

The approach developed here to obtain transition amplitudes for time-dependent potentials is generalized in the second part of this paper [1] to quantum systems with many degrees of freedom. In that paper we also show how the developed imaginary-time formalism is transformed into a real-time one, and demonstrate its applicability by treating several models.

2. Path-integral formalism for systems with time-dependent potentials

We will consider a non-relativistic quantum multi-component system in d spatial dimensions with a Hamilton operator which consists of the usual kinetic term and a time-dependent potential:

$$\hat{H}(\hat{\mathbf{p}}, \hat{\mathbf{q}}, t) = \sum_{i=1}^P \frac{\hat{\mathbf{p}}_{(i)}^2}{2M_{(i)}} + V(\hat{\mathbf{q}}, t). \quad (2.1)$$

Here P stands for the number of particles, the $P \times d$ -dimensional vectors \mathbf{q} and \mathbf{p} describe the positions and momenta of all particles, and the parenthetic subscript (i) denotes the corresponding quantity for particle i . Although in this paper we only consider single-particle systems, here we introduce many-body notation and use it in the introductory parts of sections 3 and 4 as a preparation for the second part of this paper [1], where extensions of the presented approach to many-body systems and to the real-time formalism are developed.

Note that the potential $V(\mathbf{q}, t)$ of the system is allowed to depend on the positions of all particles, and, therefore, contains implicitly all types of interactions. In practical applications the potential V usually contains, apart from the external potential, also two- and three-body interactions, but further many-body interactions can, in principle, be included as well.

The central object for studying the dynamics of such a quantum system within the path-integral formulation is the transition amplitude

$$A(\mathbf{a}, t_a; \mathbf{b}, t_b) = \langle \mathbf{b}, t_b | \hat{U}(t_a \rightarrow t_b) | \mathbf{a}, t_a \rangle. \quad (2.2)$$

Here the vectors \mathbf{a} and \mathbf{b} describe the positions of all particles at the initial and final time t_a and t_b , $|\mathbf{a}, t_a\rangle$ and $|\mathbf{b}, t_b\rangle$ denote the corresponding Hilbert-space states of the system, and

$$\hat{U}(t_a \rightarrow t_b) = \hat{T} \exp \left\{ -\frac{i}{\hbar} \int_{t_a}^{t_b} dt \hat{H}(\hat{\mathbf{p}}, \hat{\mathbf{q}}, t) \right\} \quad (2.3)$$

represents the evolution operator of the system describing its propagation from t_a to t_b . Here we assumed $t_a < t_b$ and introduced the standard time-ordering operator

$$\hat{T}\{\hat{O}(t)\hat{O}(t')\} = \begin{cases} \hat{O}(t)\hat{O}(t'), & \text{if } t > t', \\ \hat{O}(t')\hat{O}(t), & \text{otherwise.} \end{cases} \quad (2.4)$$

The starting point in setting up the path-integral formalism is the completeness relation

$$A(\mathbf{a}, t_a; \mathbf{b}, t_b) = \int d\mathbf{q}_1 \cdots \int d\mathbf{q}_{N-1} A(\mathbf{a}, t_a; \mathbf{q}_1, t_1) A(\mathbf{q}_1, t_1; \mathbf{q}_2, t_2) \cdots A(\mathbf{q}_{N-1}, t_{N-1}; \mathbf{b}, t_b), \quad (2.5)$$

where $\varepsilon = (t_b - t_a)/N$ denotes the time-slice width, $t_n = t_a + n\varepsilon$ are discrete time steps, and the $P \times d$ -dimensional vectors $\mathbf{q}_1, \dots, \mathbf{q}_{N-1}$ describe positions of all particles at a given discrete time step that is specified by the non-parenthetic index. To leading order in ε , the short-time transition amplitude reads

$$A(\mathbf{q}_n, t_n; \mathbf{q}_{n+1}, t_{n+1}) \approx \frac{1}{(2\pi\hbar i\varepsilon)^{Pd/2}} \exp \left\{ \frac{i}{\hbar} S^{(1)}(\mathbf{q}_n, t_n; \mathbf{q}_{n+1}, t_{n+1}) \right\}, \quad (2.6)$$

where the naive discretized action $S^{(1)}$ is usually expressed as

$$S^{(1)}(\mathbf{q}_n, t_n; \mathbf{q}_{n+1}, t_{n+1}) = \varepsilon \left\{ \frac{1}{2} \left(\frac{\boldsymbol{\delta}_n}{\varepsilon} \right)^2 - V(\mathbf{x}_n, \tau_n) \right\}. \quad (2.7)$$

Here we introduced the discretized velocity $\boldsymbol{\delta}_n = \mathbf{q}_{n+1} - \mathbf{q}_n$, and rescaled the coordinates so that the mass of all particles is equal to unity. The potential V is evaluated at the mid-point coordinate $\mathbf{x}_n = (\mathbf{q}_n + \mathbf{q}_{n+1})/2$ and at the mid-point time $\tau_n = (t_n + t_{n+1})/2$.

Equation (2.7) is correct to order $\varepsilon \sim 1/N$ and, therefore, after substitution into equation (2.6), leads to errors of the order $O(1/N^2)$ for discretized short-time transition amplitudes. Note that the normalization factor $\sim 1/\varepsilon^{Pd/2}$ in equation (2.6) does not affect the N -scaling of errors, since short-time amplitudes will be inserted into the completeness relation (2.5), where this normalization factor will be added to the normalization of the long-time transition amplitude. However, due to the fact that equation (2.5) contains a product of N short-time transition amplitudes, the deviation of the obtained discrete transition amplitude from the corresponding continuum result will be of the order $N \cdot O(1/N^2) = O(1/N)$. For this reason the naive discretized action is designated by $S^{(1)}$.

In the limit $N \rightarrow \infty$ we recover the continuous transition amplitude, which leads to the formal coordinate-space path-integral expression

$$A(\mathbf{a}, t_a; \mathbf{b}, t_b) = \int_{\mathbf{q}(t_a)=\mathbf{a}}^{\mathbf{q}(t_b)=\mathbf{b}} \mathcal{D}\mathbf{q}(t) \exp \left\{ \frac{i}{\hbar} S[\mathbf{q}] \right\}, \quad (2.8)$$

where the integration is defined over all possible trajectories $\mathbf{q}(t)$ through the discretization process described above. In this equation, the action S for a given trajectory $\mathbf{q}(t)$ is defined as usual:

$$S[\mathbf{q}] = \int_{t_a}^{t_b} dt \left\{ \frac{1}{2} \dot{\mathbf{q}}^2(t) - V(\mathbf{q}(t), t) \right\}. \quad (2.9)$$

The derivation outlined represents the basis for the path-integral formulation of quantum mechanics [21], [60]–[62] as well as for the numerical calculation of path integrals. The described discretization procedure is most straightforwardly numerically implemented by the path-integral Monte Carlo approach [63].

Note that the $O(1/N)$ convergence can be also achieved with other choices of space–time points at which we evaluate the potential in equation (2.7). For example, the left or the right prescription $\mathbf{x}_n = \mathbf{q}_n, \tau_n = t_n$ or $\mathbf{x}_n = \mathbf{q}_{n+1}, \tau_{n+1} = t_{n+1}$ is often used for the spatio-temporal argument of the potential. These different choices affect neither the numerical calculation nor the analytical derivation, and different prescriptions can even be translated into each other. However, it turns out that the mid-point prescription always yields the simplest analytic results, and, therefore, we will use it throughout this paper.

In the following we will switch to the imaginary-time formalism, which is widely used in numerical simulations [63], since it mitigates problems that are related to the oscillatory nature of the integrand in the real-time approach. To obtain the real-time from the imaginary-time amplitudes, one would have to perform an inverse Wick rotation, i.e. a suitable analytic continuation of the numerical results. This might be difficult due to the inherent instability of this procedure with respect to statistical noise, which is always present in numerical calculations. However, using the imaginary time is justified by the fact that all current applications of this approach are related to quantum statistical physics, which is naturally set up in imaginary time, with the inverse temperature $\beta = 1/k_B T$ playing the role of the imaginary time. Also, energy spectra and energy eigenfunctions can be efficiently calculated in this formalism [50, 51]. Note that the derived analytic expressions for higher-order propagators can be formally transformed from the imaginary- to the real-time axis. In the next paper [1], we will demonstrate by treating

several simple examples that such analytic expressions can be successfully used to calculate the real-time evolution in the context of the space-discretized approach [50, 51].

After Wick rotation to the imaginary time, the transition amplitude is expressed as

$$A(\mathbf{a}, t_a; \mathbf{b}, t_b) = \int_{\mathbf{q}(t_a)=\mathbf{a}}^{\mathbf{q}(t_b)=\mathbf{b}} \mathcal{D}\mathbf{q}(t) e^{-(1/\hbar)S_E[\mathbf{q}]}, \quad (2.10)$$

where the action is replaced by its imaginary-time counterpart, the Euclidean action

$$S_E[\mathbf{q}] = \int_{t_a}^{t_b} dt \left\{ \frac{1}{2} \dot{\mathbf{q}}^2(t) + V(\mathbf{q}(t), t) \right\}, \quad (2.11)$$

which represents the energy of the system. To simplify the notation, we will drop the subscript E from now on. If we consider in equation (2.10) only diagonal amplitudes, i.e. $\mathbf{a} = \mathbf{b}$, and integrate over \mathbf{a} , we obtain the path-integral expression for the partition function

$$Z(\beta) = \text{Tr} \left\{ \hat{T} \exp \left[-\frac{1}{\hbar} \int_0^{\hbar\beta} dt \hat{H}(t) \right] \right\} \quad (2.12)$$

by setting $t_a = 0$ and $t_b = \hbar\beta$.

3. Path-integral calculation of the propagator

In this paper we develop a method for calculating short-time transition amplitudes for time-dependent potentials to high orders in the propagation time. To this end we follow the approach of [48] and generalize the level $p = 1$ discretized transition amplitude from equation (2.6) in such a way that the exact transition amplitude is written as

$$A(\mathbf{a}, t_a; \mathbf{b}, t_b) = \frac{1}{(2\pi\varepsilon)^{Pd/2}} e^{-S^*(\mathbf{x}, \boldsymbol{\delta}; \varepsilon, \tau)}. \quad (3.1)$$

Here we use the convention $\hbar = 1$, the ideal discretized effective action reads [59, 64]

$$S^*(\mathbf{x}, \boldsymbol{\delta}; \varepsilon, \tau) = \frac{\boldsymbol{\delta}^2}{2\varepsilon} + \varepsilon W(\mathbf{x}, \boldsymbol{\delta}; \varepsilon, \tau), \quad (3.2)$$

and W represents the ideal effective potential, which ensures the exactness of the above expression. The latter depends not only on the coordinate mid-point $\mathbf{x} = (\mathbf{a} + \mathbf{b})/2$, the discretized velocity $\boldsymbol{\delta} = \mathbf{b} - \mathbf{a}$, and the time interval $\varepsilon = t_b - t_a$ as already introduced in the case for time-independent potentials, but also on the time mid-point $\tau = (t_a + t_b)/2$, due to the explicit time dependence of the potential.

We will analytically derive a systematic short-time expansion of the effective potential W , which provides an improved convergence for numerically calculating transition amplitudes and partition functions as well as other properties of quantum systems with time-dependent potentials. The expansion of the effective potential W to order ε^{p-1} yields the effective action correct to order ε^p , with errors proportional to ε^{p+1} . Due to the normalization factor in the expression (3.1), the total ε -convergence of the amplitude is given by

$$A_p(\mathbf{a}, t_a; \mathbf{b}, t_b) = A(\mathbf{a}, t_a; \mathbf{b}, t_b) + O(\varepsilon^{p+1-Pd/2}). \quad (3.3)$$

This ε -scaling of errors is valid if we are interested in calculating short-time transition amplitudes, which is the main objective of this paper. However, if we use such short-time transition amplitudes to calculate long-time transition amplitudes through the time-discretization procedure (2.5), due to successive integrals the normalization factors will again be added, and we will get total errors of the order $N \cdot O(1/N^{p+1}) = O(1/N^p)$. Although the corresponding effective actions and resulting discretized short-time transition amplitudes are designated by the index p according to their N -scaling behavior, we stress that the scaling with respect to the short propagation time is always given by equation (3.3).

Before we embark upon developing a systematic recursive approach for analytically calculating higher-order effective actions, we first have to study the general structure of the effective potential, which turns out to be more complex than in the case of time-independent quantum systems. In order to do so, we calculate the short-time expansion of the effective potential by using an *ab initio* approach introduced in [47]. To simplify the calculation, we will restrict ourselves in the present section to the single-particle one-dimensional case. Based on these results we will develop in section 5 the systematic recursive approach for such simple quantum systems, and then extend and generalize this procedure to systems with many degrees of freedom.

Following [47], we start by changing the variables via $q(t) = \xi(t) + y(t)$, where $\xi(t)$ is some chosen reference trajectory satisfying the same boundary conditions as the path $q(t)$, i.e. $\xi(t_a) = a$, $\xi(t_b) = b$. This implies that the new variable $y(t)$ vanishes at the boundaries, i.e. $y(t_a) = y(t_b) = 0$. We also introduce a new time variable s by $t = \tau + s$, in which the boundaries are defined by $s_a = -\varepsilon/2$, $s_b = \varepsilon/2$. In the new variables, the kinetic energy functional has the form

$$\int_{t_a}^{t_b} dt \frac{1}{2} \left(\frac{dq(t)}{dt} \right)^2 = \int_{-\varepsilon/2}^{\varepsilon/2} ds \left\{ \frac{1}{2} \dot{\xi}^2(s) + \frac{1}{2} \dot{y}^2(s) - y(s) \ddot{\xi}(s) \right\}, \quad (3.4)$$

where a dot represents a derivative with respect to the time s . With this the transition amplitude reads

$$A(a, t_a; b, t_b) = e^{-S[\xi](\tau)} \int_{y(-\varepsilon/2)=0}^{y(\varepsilon/2)=0} \mathcal{D}y(s) e^{-\int_{-\varepsilon/2}^{\varepsilon/2} ds \left\{ (1/2) \dot{y}^2(s) + U_\xi(y(s), s) \right\}}, \quad (3.5)$$

where the quantity U_ξ is defined as

$$U_\xi(y(s), s) = V(\xi(s) + y(s), \tau + s) - V(\xi(s), \tau) - y(s) \ddot{\xi}(s), \quad (3.6)$$

and the Euclidean action $S[\xi](\tau)$ for the reference trajectory $\xi(s)$ is defined by an expression similar to equation (2.11), but with the time argument of the potential being fixed now by the mid-point τ :

$$S[\xi](\tau) = \int_{-\varepsilon/2}^{\varepsilon/2} ds \left\{ \frac{1}{2} \dot{\xi}^2(s) + V(\xi(s), \tau) \right\}. \quad (3.7)$$

Thus, the transition amplitude reads

$$A(a, t_a; b, t_b) = \frac{e^{-S[\xi](\tau)}}{\sqrt{2\pi\varepsilon}} \langle e^{-\int_{-\varepsilon/2}^{\varepsilon/2} ds U_\xi(y(s), s)} \rangle, \quad (3.8)$$

where the path-integral expectation value is defined with respect to the free-particle action:

$$\langle \bullet \rangle = \sqrt{2\pi\varepsilon} \int_{y(-\varepsilon/2)=0}^{y(\varepsilon/2)=0} \mathcal{D}y(s) \bullet e^{-\int_{-\varepsilon/2}^{\varepsilon/2} ds (1/2)\dot{y}^2(s)}. \quad (3.9)$$

The transition amplitude (3.8) can then be obtained through a standard calculation of the free-particle expectation value by using the Taylor expansion

$$\begin{aligned} \langle e^{-\int_{-\varepsilon/2}^{\varepsilon/2} ds U_\xi(y(s), s)} \rangle &= 1 - \int_{-\varepsilon/2}^{\varepsilon/2} ds \langle U_\xi(y(s), s) \rangle \\ &+ \frac{1}{2} \int_{-\varepsilon/2}^{\varepsilon/2} ds \int_{-\varepsilon/2}^{\varepsilon/2} ds' \langle U_\xi(y(s), s) U_\xi(y(s'), s') \rangle + \dots \end{aligned} \quad (3.10)$$

As we see from equation (3.6), the quantity U_ξ has the simplest form if we choose the reference trajectory ξ in such a way that its second derivative with respect to the time s vanishes. The natural choice is thus the linear trajectory

$$\xi(s) = x + s\delta/\varepsilon,$$

centered around the mid-point $x = (a+b)/2$. In order to calculate the expectation values in equation (3.10), we further have to expand

$$U_\xi(y(s), s) = V(\xi(s) + y(s), \tau + s) - V(\xi(s), \tau) \quad (3.11)$$

around this reference trajectory according to

$$U_\xi(y(s), s) = \sum_{\substack{n,m=0 \\ n+m>0}}^{\infty} \frac{1}{n! m!} V^{(m)(n)}(\xi(s), \tau) y^n(s) s^m, \quad (3.12)$$

where, in order to simplify the notation, (m) denotes the order of the partial derivative with respect to the time s , and (n) denotes the order of the partial derivative with respect to the spatial coordinate. For a free-particle theory, expectation values of the type $\langle y^{n_1}(s_1) y^{n_2}(s_2) \dots \rangle$ can be easily calculated using the standard generating functional approach. The expectation value $\langle y(s) \rangle$ vanishes due to the symmetry, while the correlator $\Delta(s, s') = \langle y(s) y(s') \rangle$ is given by the expression

$$\Delta(s, s') = \frac{\theta(s - s')}{\varepsilon} \left(\frac{\varepsilon}{2} - s \right) \left(\frac{\varepsilon}{2} + s' \right) + (s \leftrightarrow s'), \quad (3.13)$$

and higher expectation values can be found in [47].

In order to obtain an expansion of the transition amplitude in the propagation time ε , one has to consider equation (3.10) and to take into account the powers of ε of all terms to identify the relevant terms at the desired level p . To illustrate this, let us look at the term linear in U_ξ

$$\int_{-\varepsilon/2}^{\varepsilon/2} ds \langle U_\xi(y(s), s) \rangle = \int_{-\varepsilon/2}^{\varepsilon/2} ds \sum_{\substack{n,m=0 \\ n+m>0}}^{\infty} \frac{1}{n! m!} V^{(m)(n)}(\xi(s), \tau) \langle y^n(s) \rangle s^m, \quad (3.14)$$

where the integration over s yields terms proportional to ε^{m+1} times the contribution of the expectation value term. For example, from equation (3.13) we see that the

$n = 2$ expectation value would yield an additional ε power, amounting to a total ε^{m+2} dependence of the term corresponding to a given m and $n = 2$. Since we are interested in calculating all terms to a given order in ε , we have to carefully inspect all possible terms and to select the appropriate ones at a given level p . As an example we write down all terms which contribute to the expectation value (3.10) to order $O(\varepsilon^4)$:

$$\begin{aligned} \langle e^{-\int_{-\varepsilon/2}^{\varepsilon/2} ds U_{\xi}(y(s),s)} \rangle &= 1 - \int_{-\varepsilon/2}^{\varepsilon/2} ds \left\{ \frac{1}{2} V''(\xi(s), \tau) \langle y^2(s) \rangle + \frac{1}{24} V^{(4)}(\xi(s), \tau) \langle y^4(s) \rangle \right. \\ &\quad + \dot{V}(\xi(s), \tau) s + \frac{1}{2} \dot{V}^{(2)}(\xi(s), \tau) \langle y^2(s) \rangle s + \frac{1}{2} \ddot{V}(\xi(s), \tau) s^2 \left. \right\} \\ &\quad + \frac{1}{2} \int_{-\varepsilon/2}^{\varepsilon/2} ds \int_{-\varepsilon/2}^{\varepsilon/2} ds' V'(\xi(s), \tau) V'(\xi(s'), \tau) \langle y(s) y(s') \rangle + O(\varepsilon^4). \end{aligned} \quad (3.15)$$

In the above expression, the correlators $\langle y^2(s) \rangle = \Delta(s, s)$ and $\langle y(s) y(s') \rangle = \Delta(s, s')$ are given by equation (3.13), and the expectation value $\langle y^4(s) \rangle$ can be directly determined using either the generating functional method or the Wick rule, yielding $3\Delta^2(s, s)$. In order to be able to calculate the remaining integrals over s and s' , we need to expand also the potential V and its derivatives with respect to the first argument $\xi(s) = x + s\delta/\varepsilon$ around the mid-point x . The required number of terms in this expansion, contributing to the desired order of ε , is obtained by taking into account the diffusion relation $\delta^2 \sim \varepsilon$, which is valid for small propagation times ε and has been demonstrated to yield a consistent expansion of short-time transition amplitudes [48]. The expansion of the potential into a power series in $s\delta/\varepsilon$ gives an additional polynomial s -dependence, which finally allows an analytic calculation of all the integrals in equation (3.15). When this is done, we obtain the following expression for the expectation value (3.10)

$$\begin{aligned} \langle e^{-\int_{-\varepsilon/2}^{\varepsilon/2} ds U_{\xi}(y(s),s)} \rangle &= 1 - V'' \frac{\varepsilon^2}{12} - \dot{V}' \frac{\delta \varepsilon^2}{12} - V^{(4)} \frac{\varepsilon^3}{240} - \ddot{V} \frac{\varepsilon^3}{24} + V'^2 \frac{\varepsilon^3}{24} - V^{(4)} \frac{\delta^2 \varepsilon^2}{480} \\ &\quad - \dot{V}^{(3)} \frac{\delta \varepsilon^3}{240} - \dot{V}^{(3)} \frac{\delta^3 \varepsilon^2}{480} + O(\varepsilon^4), \end{aligned} \quad (3.16)$$

where the potential V as well as its spatial and temporal derivatives are evaluated at the mid-point x, τ , i.e. $V = V(x, \tau)$. Note that we have retained in equation (3.16) only those terms whose order is less than ε^4 . Taking into account the diffusion relation $\delta^2 \sim \varepsilon$, the terms proportional to ε^3 and $\delta^2 \varepsilon^2$ are considered to be of the same order.

Combining equations (3.1) and (3.8), we see that the ideal effective action can be expressed by its short-time expression (3.7) and the expectation value (3.10) according to

$$S^*(x, \delta; \varepsilon, \tau) = S[\xi](\tau) - \log \langle e^{-\int_{-\varepsilon/2}^{\varepsilon/2} ds U_{\xi}(y(s),s)} \rangle. \quad (3.17)$$

After expanding the potential V around the mid-point x in the action $S[\xi](\tau)$ in equation (3.7), we obtain its short-time expansion:

$$S[\xi](\tau) = \frac{\delta^2}{2\varepsilon} + V\varepsilon + V'' \frac{\delta^2 \varepsilon}{24} + V^{(4)} \frac{\delta^4 \varepsilon}{1920} + O(\varepsilon^4). \quad (3.18)$$

This allows us to calculate the short-time expansion of the effective potential W from equations (3.2) and (3.16)–(3.18). For example, up to level $p = 3$ we get

$$W_3(x, \delta; \varepsilon, \tau) = V + V'' \frac{\varepsilon}{12} + V''' \frac{\delta^2}{24} + \dot{V}' \frac{\delta \varepsilon}{12} + V^{(4)} \frac{\varepsilon^2}{240} + \ddot{V} \frac{\varepsilon^2}{24} - V'^2 \frac{\varepsilon^2}{24} + V^{(4)} \frac{\delta^2 \varepsilon}{480} + V^{(4)} \frac{\delta^4}{1920}. \quad (3.19)$$

Numerically, such a result allows the faster calculation of the transition amplitudes, since the errors can be substantially reduced using analytic expressions for higher-level effective actions.

Compared to our previous results for the effective actions of time-independent potentials V in [48], we see that new terms appear that contain time derivatives of the potential. In particular, we observe the emergence of terms with odd powers of the discretized velocity δ , which was previously not the case. In fact, for time-independent potentials we have shown in [48] that the effective potential is symmetric in δ , which leaves only even powers of δ in its short-time expansion. Here, however, also odd powers of δ survive due to the explicit time dependence of the potential. We also recognize that all new terms are proportional to time derivatives of the potential and vanish in the time-independent case, thus reducing the effective action to the previous expressions in [48].

Therefore, the correct systematic short-time expansion of the effective potential turns out to have the form

$$W(x, \delta; \varepsilon, \tau) = \sum_{m=0}^{\infty} \sum_{k=0}^m \left\{ c_{m,k}(x, \tau) \varepsilon^{m-k} \left(\frac{\delta}{2} \right)^{2k} + c_{m+1/2,k}(x, \tau) \varepsilon^{m-k} \left(\frac{\delta}{2} \right)^{2k+1} \right\}. \quad (3.20)$$

Here $\delta/2$ is used as the expansion parameter in order to have expansion coefficients c which are defined consistently with [48]. Such an expansion allows the level p effective action to be written as the sum of terms corresponding to $m = 0, 1, \dots, p-1$. Note that for $m = p-1$ we need to take into account only the even-power terms $c_{p-1,k}(x, \tau) \varepsilon^{p-1-k} (\delta/2)^{2k}$. The odd-power terms $c_{p-1/2,k}(x, \tau) \varepsilon^{p-1-k} (\delta/2)^{2k+1}$ are proportional to $\varepsilon^{p-1/2}$, i.e. they are of higher order than the required ε^{p-1} for level p effective action. For this reason, the correct expansion of the effective potential at level p is given by

$$W_p(x, \delta; \varepsilon, \tau) = \sum_{m=0}^{p-1} \sum_{k=0}^m c_{m,k}(x, \tau) \varepsilon^{m-k} \left(\frac{\delta}{2} \right)^{2k} + \sum_{m=0}^{p-2} \sum_{k=0}^m c_{m+1/2,k}(x, \tau) \varepsilon^{m-k} \left(\frac{\delta}{2} \right)^{2k+1}, \quad (3.21)$$

and it provides the convergence of transition amplitudes according to equation (3.3).

4. Forward and backward Schrödinger equation

In this and in section 5 we will use the latter result (3.20) to develop a systematic recursive approach for analytically calculating effective actions to high levels p for time-dependent potentials. To this end, in this section we rederive both the forward and the backward Schrödinger equation for the transition amplitude and then use them to derive corresponding differential equations for the effective potential W . Afterward, in section 5

we use equation (3.20) to solve the derived equations for W and to obtain recursion relations for single-particle one-dimensional systems.

The evolution operator for a quantum system in a time-dependent potential is given by equation (2.3), or, in imaginary time,

$$\hat{U}(t_a \rightarrow t_b) = \hat{T} \exp \left\{ - \int_{t_a}^{t_b} dt \hat{H}(\hat{\mathbf{p}}, \hat{\mathbf{q}}, t) \right\}. \quad (4.1)$$

Thus, the evolution operator obeys the differential equation

$$\partial_{t_b} \hat{U}(t_a \rightarrow t_b) = -\hat{H}(\hat{\mathbf{p}}, \hat{\mathbf{q}}, t_b) \hat{U}(t_a \rightarrow t_b), \quad (4.2)$$

and, similarly,

$$\partial_{t_a} \hat{U}(t_a \rightarrow t_b) = \hat{U}(t_a \rightarrow t_b) \hat{H}(\hat{\mathbf{p}}, \hat{\mathbf{q}}, t_a). \quad (4.3)$$

If we determine from equation (4.2) the matrix elements which correspond to the transition amplitude equation (2.2), we obtain the forward Schrödinger equation for the transition amplitude

$$\partial_{t_b} A(\mathbf{a}, t_a; \mathbf{b}, t_b) = -\hat{H}_b A(\mathbf{a}, t_a; \mathbf{b}, t_b), \quad (4.4)$$

where \hat{H}_b stands for the coordinate-space Hamilton operator $\hat{H}_b = H(-i\partial_{\mathbf{b}}, \mathbf{b}, t_b)$, in which momentum and position operators are replaced by their coordinate-space representations at \mathbf{b} . To obtain the analogous equation for the derivative with respect to the initial time t_a , we have to take into account that the imaginary-time transition amplitudes as well as its time derivative are real. With this equation (4.3) yields at first

$$\langle \mathbf{b} | \partial_{t_a} \hat{U}(t_a \rightarrow t_b) | \mathbf{a} \rangle = H(-i\partial_{\mathbf{a}}, \mathbf{a}, t_a) \langle \mathbf{a} | \hat{U}^\dagger(t_a \rightarrow t_b) | \mathbf{b} \rangle. \quad (4.5)$$

Since we have in addition

$$\langle \mathbf{a} | \hat{U}^\dagger(t_a \rightarrow t_b) | \mathbf{b} \rangle = A(\mathbf{a}, t_a; \mathbf{b}, t_b), \quad (4.6)$$

we finally get the backward Schrödinger equation for the transition amplitude

$$\partial_{t_a} A(\mathbf{a}, t_a; \mathbf{b}, t_b) = \hat{H}_a A(\mathbf{a}, t_a; \mathbf{b}, t_b), \quad (4.7)$$

where $\hat{H}_a = H(-i\partial_{\mathbf{a}}, \mathbf{a}, t_a)$ is defined analogously as \hat{H}_b .

In the next step we change the original time variables t_a and t_b to the mid-point τ and the propagation time ε , which converts (4.4) and (4.7) to

$$[\partial_\varepsilon + \frac{1}{2}(\hat{H}_a + \hat{H}_b)] A(\mathbf{a}, t_a; \mathbf{b}, t_b) = 0, \quad (4.8)$$

$$[\partial_\tau + (\hat{H}_b - \hat{H}_a)] A(\mathbf{a}, t_a; \mathbf{b}, t_b) = 0. \quad (4.9)$$

Subsequently, we also change the spatial variables \mathbf{a} and \mathbf{b} to the mid-point \mathbf{x} and the discretized velocity $\bar{\mathbf{x}} = \boldsymbol{\delta}/2$, thus equations (4.8) and (4.9) then read

$$[\partial_\varepsilon - \frac{1}{8} \partial^2 - \frac{1}{8} \bar{\partial}^2 + \frac{1}{2}(V_+ + V_-)] A(\mathbf{x}, \bar{\mathbf{x}}; \varepsilon, \tau) = 0, \quad (4.10)$$

$$[\partial_\tau - \frac{1}{2} \partial \bar{\partial} + V_+ - V_-] A(\mathbf{x}, \bar{\mathbf{x}}; \varepsilon, \tau) = 0, \quad (4.11)$$

where we have introduced $V_\pm = V(\mathbf{x} \pm \bar{\mathbf{x}}, \tau \pm \varepsilon/2)$ as abbreviations, and the $P \times d$ -dimensional Laplacians $\partial_{\mathbf{x}} \cdot \partial_{\mathbf{x}} = \partial^2$ over coordinates \mathbf{x} and $\partial_{\bar{\mathbf{x}}} \cdot \partial_{\bar{\mathbf{x}}} = \bar{\partial}^2$ over coordinates

$\bar{\mathbf{x}}$, as well as the mixed Laplacian $\partial_{\mathbf{x}} \cdot \partial_{\bar{\mathbf{x}}} = \partial \bar{\partial}$. Note that we will not use equation (4.11) in our further calculation of the short-time transition amplitude. This equation describes the dynamics caused only by the presence of the explicit time dependence of the potential, as is indicated by the derivative with respect to the time mid-point τ .

If we now express the transition amplitude (3.1) by using the effective potential in (3.2) and the new spatio-temporal variables, we get

$$A(\mathbf{x}, \bar{\mathbf{x}}; \varepsilon, \tau) = \frac{1}{(2\pi\varepsilon)^{Pd/2}} e^{-(2/\varepsilon)\bar{\mathbf{x}}^2 - \varepsilon W(\mathbf{x}, \bar{\mathbf{x}}; \varepsilon, \tau)}. \quad (4.12)$$

Substituting this expression into the differential equation for the transition amplitude (4.10), we obtain a corresponding differential equation for the effective potential:

$$W + \bar{\mathbf{x}} \cdot \bar{\partial} W + \varepsilon \partial_{\varepsilon} W - \frac{1}{8} \varepsilon \partial^2 W - \frac{1}{8} \varepsilon \bar{\partial}^2 W + \frac{1}{8} \varepsilon^2 (\partial W)^2 + \frac{1}{8} \varepsilon^2 (\bar{\partial} W)^2 = \frac{1}{2} (V_+ + V_-). \quad (4.13)$$

This equation is formally identical to the corresponding equation (29) from [48], and in the limit of the time-independent potential we recover the previously derived result. Equation (4.13) can now be used to develop a recursive approach for calculating the effective potential W by using the double-power series (3.20) in both ε and $\bar{\mathbf{x}}$.

5. Recursive calculation of the propagator for one-dimensional systems

In this section we consider a single-particle one-dimensional system in a given external time-dependent potential V , and fully develop a recursive approach for calculation of the short-time expansion of the effective potential W . In this case, the right-hand-side of equation (4.13) can be expanded in a double-power series of the form

$$\frac{1}{2} (V_+ + V_-) = \frac{1}{2} \sum_{k, m \geq 0}^{\infty} \frac{1}{k! m!} V^{(m)}{}^{(k)} \left(\frac{\varepsilon}{2}\right)^m \bar{x}^k \{1 + (-1)^{m+k}\}. \quad (5.1)$$

We see that m and k must be of the same parity in order to yield a non-zero contribution. Therefore, we introduce the quantity $\Pi(m, k)$, which is equal to one if $m - k$ is even, and vanishes otherwise. This allows us to reorganize terms of the double-power series (5.1) in a form which corresponds to the expansion of the effective potential in equation (3.20):

$$\begin{aligned} \frac{1}{2} (V_+ + V_-) = & \sum_{m=0}^{\infty} \sum_{k=0}^m \left\{ \frac{\Pi(m, k) \varepsilon^{m-k} \bar{x}^{2k}}{(2k)! (m-k)! 2^{m-k}} V^{(m-k)}{}^{(2k)} \right. \\ & \left. + \frac{[1 - \Pi(m, k)] \varepsilon^{m-k} \bar{x}^{2k+1}}{(2k+1)! (m-k)! 2^{m-k}} V^{(m-k)}{}^{(2k+1)} \right\}. \end{aligned} \quad (5.2)$$

In order to solve equation (4.13) with (5.2), we now substitute the effective potential W with its double expansion (3.20). By comparing terms with even and odd powers of \bar{x} , we obtain algebraic equations which determine the coefficients $c_{m,k}$ and $c_{m+1/2,k}$. After a

straightforward calculation we get

$$\begin{aligned}
8(m+k+1)c_{m,k} &= 8 \frac{\Pi(m,k) V^{(m-k)(2k)}}{(2k)!(m-k)!2^{m-k}} + (2k+2)(2k+1)c_{m,k+1} + c''_{m-1,k} \\
&\quad - \sum_{l,r} \{c'_{l,r} c'_{m-l-2,k-r} + c'_{l+1/2,r} c'_{m-l-5/2,k-r-1} \\
&\quad + 2r(2k-2r+2)c_{l,r}c_{m-l-1,k-r+1} \\
&\quad + (2r+1)(2k-2r+1)c_{l+1/2,r}c_{m-l-3/2,k-r}\}, \tag{5.3}
\end{aligned}$$

$$\begin{aligned}
8(m+k+2)c_{m+1/2,k} &= 8 \frac{[1-\Pi(m,k)] V^{(m-k)(2k+1)}}{(2k+1)!(m-k)!2^{m-k}} + (2k+3)(2k+2)c_{m+1/2,k+1} \\
&\quad + c''_{m-1/2,k} - \sum_{l,r} \{c'_{l,r} c'_{m-l-3/2,k-r} + c'_{l+1/2,r} c'_{m-l-2,k-r} \\
&\quad + (2r+1)(2k-2r+2)c_{l+1/2,r}c_{m-l-1,k-r+1} \\
&\quad + 2r(2k-2r+3)c_{l,r}c_{m-l-1/2,k-r+1}\}. \tag{5.4}
\end{aligned}$$

In the above relations, sums over l and r are restricted by the non-negativity of indices for both even- and odd-power coefficients c . It is immediately seen in the case of a time-independent potential that the recursion for even-power coefficients $c_{m,k}$ in equation (5.3) reduces to the previously derived recursion of [48], while the odd-power recursion (5.4) automatically renders all coefficients $c_{m+1/2,k}$ to be zero.

In order to efficiently solve these algebraic equations at a given level p , we recall the corresponding hierarchical level p expansion (3.21). In such an expansion, we look only for even-power coefficients $c_{m,k}$ with $0 \leq m \leq p-1$, and odd-power coefficients $c_{m+1/2,k}$ with $0 \leq m \leq p-2$, while the index k is always restricted by $0 \leq k \leq m$. To simplify the calculation, we formally set all the coefficients with higher values of indices to zero. As in the case for a time-independent potential in [48], we are then able to calculate explicitly diagonal even-order coefficients $c_{m,m}$ for any m :

$$c_{m,m} = \frac{V^{(2m)}}{(2m+1)!}. \tag{5.5}$$

Correspondingly, we obtain for the diagonal odd-power coefficients the general result is

$$c_{m+1/2,m} = 0. \tag{5.6}$$

Thus, the recursion relations (5.3) and (5.4) represent, together with (5.5) and (5.6), a closed set of algebraic equations, which completely determines the coefficients c for the effective potential at a given level p .

To illustrate how the recursive procedure works in detail, we solve the single-particle recursive relations up to order $p=3$ and demonstrate that we obtain the same result (3.19) as in section 4, where we used the path-integral approach to calculate the effective potential. For the level $p=3$ we need coefficients c with the first index m in the range $0, \dots, p-1$, i.e. $m=0, 1, 2$. For a given $m \leq p-1$ we start by calculating even-power coefficients $c_{m,k}$ using the recursive relation (5.3) in the order $k=m, m-1, \dots, 0$, where we take into account (5.5). Then we proceed with the calculation of odd-power

coefficients $c_{m+1/2,k}$ by using equation (5.4) for the order $k = m - 1, \dots, 0$ and by taking into account (5.6). We also recall that odd-power coefficients need not be calculated for $m = p - 1$, i.e. in the last step of the recursive procedure for $m = p - 1$ we only calculate even-power coefficients. Following this procedure, we immediately get from (5.5) for $m = 0$

$$c_{0,0} = V. \quad (5.7)$$

The coefficient $c_{1/2,0} = 0$ follows trivially from (5.6). For $m = 1$ we get the following even-power coefficients, corresponding to the values $k = 1$ and 0:

$$c_{1,1} = \frac{1}{6}V'', \quad (5.8)$$

$$c_{1,0} = \frac{1}{16}c''_{0,0} + \frac{1}{8}c_{1,1} = \frac{1}{12}V''. \quad (5.9)$$

For the only non-trivial $m = 1$ odd-power coefficient $c_{3/2,0}$ we get

$$c_{3/2,0} = \frac{1}{4}c_{3/2,1} + \frac{1}{24}c''_{1/2,0} + \frac{1}{6}\dot{V}' = \frac{1}{6}\dot{V}'. \quad (5.10)$$

Similarly, we find the $m = 2$ even-power coefficients by using equations (5.3) and (5.5):

$$c_{2,2} = \frac{1}{120}V^{(4)}, \quad (5.11)$$

$$c_{2,1} = \frac{1}{32}c''_{1,1} + \frac{3}{8}c_{2,2} = \frac{1}{120}V^{(4)}, \quad (5.12)$$

$$c_{2,0} = \frac{1}{24}\ddot{V} - \frac{1}{24}c'^2_{0,0} + \frac{1}{24}c''_{1,0} + \frac{1}{12}c_{2,1} = \frac{1}{24}\ddot{V} + \frac{1}{240}V^{(4)} - \frac{1}{24}V'^2. \quad (5.13)$$

This result is already sufficient to construct the effective potential $W_{p=3}$. If we insert the calculated coefficients in the expansion (3.21) at the given level $p = 3$, we reobtain the same expression as in equation (3.19). Comparing the calculated even-power coefficients $c_{m,k}$ with the previously calculated ones for the time-independent potential in [48], we see that they coincide if we set all time derivatives of the potential to zero, as expected, and that all odd-power coefficients vanish.

We stress that the recursive approach is far more efficient than the path-integral calculation presented in section 4. For example, if one wants to extend a level p calculation to a higher order $p' = p + 1$, this requires in the path-integral approach not only to take into account the next term in the expansion (3.15), but also each previously calculated expectation value term has to be redone to one order in ε higher. The complexity of this algorithm prevents its efficient implementation. However, in the present recursive approach, all we need to do is to calculate one additional order of odd-power coefficients $c_{p-1/2,k}$, which corresponds to $m = p' - 2 = p - 1$, and even-power coefficients $c_{p,k}$, which corresponds to $m = p' - 1 = p$. To do this, we just apply the recursive relations and use the previously calculated lower-order coefficients c . For instance, in order to obtain level $p' = 4$, we proceed first by calculating $m = p' - 2 = 2$ odd-power coefficients $c_{5/2,k}$. The highest coefficient $c_{5/2,2} = 0$ is automatically equal to zero due to (5.6), while for lower-level coefficients we get

$$c_{5/2,1} = \frac{1}{2}c_{5/2,2} + \frac{1}{40}c''_{3/2,1} + \frac{1}{60}\dot{V}^{(3)} = \frac{1}{60}\dot{V}^{(3)}, \quad (5.14)$$

$$c_{5/2,0} = \frac{3}{16}c_{5/2,1} + \frac{1}{32}c''_{3/2,0} - \frac{1}{16}c'_{1/2,0}c'_{0,0} - \frac{1}{8}c_{1/2,0}c_{1,1} = \frac{1}{120}\dot{V}^{(3)}. \quad (5.15)$$

To completely determine the $p' = 4$ effective action, we then calculate even-power $m = p' - 1 = 3$ coefficients $c_{3,k}$, and obtain from equations (5.3) and (5.5)

$$c_{3,3} = \frac{1}{5040} V^{(6)}, \quad (5.16)$$

$$c_{3,2} = \frac{1}{3360} V^{(6)}, \quad (5.17)$$

$$c_{3,1} = \frac{1}{3360} V^{(6)} + \frac{1}{80} \dot{V}'' - \frac{1}{360} V''^2 - \frac{1}{120} V' V^{(3)}, \quad (5.18)$$

$$c_{3,0} = \frac{1}{6720} V^{(6)} + \frac{1}{480} \dot{V}'' - \frac{1}{360} V''^2 - \frac{1}{120} V' V^{(3)}. \quad (5.19)$$

The outlined procedure continues in the same way for higher levels p . We have automatized this procedure and implemented it in our SPEEDUP code [65] using the Mathematica 7.0 package [66] for symbolic calculus. Using this we have determined the effective action for a one-dimensional particle in a general time-dependent potential up to the level $p = 20$. Such a calculation requires around 2 GB of memory and approximately 1.5 h of CPU time on a 2.33 GHz Intel Xeon E5345 processor. Although the effective actions grow in complexity with level p , the Schrödinger equation method for calculating the discrete time effective actions turns out to be extremely efficient. The value of $p = 20$ far surpasses the previously obtained best result known in the literature for $p = 6$ [38], and is limited practically only by the sheer size of the expression for the effective action of a general theory at such a high level. The whole technique can even be pushed much further when working on specific potential classes such as, for instance, polynomial potentials, where higher spatial and temporal derivatives have a simple form. However, if this is not the case, the obtained general expressions for the effective potential can be used for any given potential.

In practical applications, the increasing complexity of expressions for higher-level effective actions leads to a corresponding increase in the necessary computation time. For levels $p \lesssim 10$ [45, 46], the increase in the computation time is minimal compared to the obtained decrease in the error of numerically calculated transition amplitudes, thus it can be used to speed up the calculation at a given level of accuracy. However, for higher values of p the error may be more efficiently reduced by decreasing the time step, i.e. by using a larger number of Monte Carlo discretization steps. Since the complexity of effective actions strongly depends on the concrete form of the given potential, the optimal values of both the level p and the size of the time step have to be estimated from a series of scaled-down numerical simulations. For example, level $p = 21$ and a certain time step have turned out to be optimal for studying fast-rotating Bose–Einstein condensates in an anharmonic trapping potential [52].

We will generalize the presented approach to many-body systems in the next paper [1], which will also include generalization of the imaginary-time to the real-time formalism, suitable for the study of dynamics of quantum systems.

6. Numerical verification

In order to numerically verify the derived analytical results, we have studied several simple models with time-dependent potentials. We have used the modified version of the Monte Carlo SPEEDUP [65] code, which implements higher-order effective actions in the C

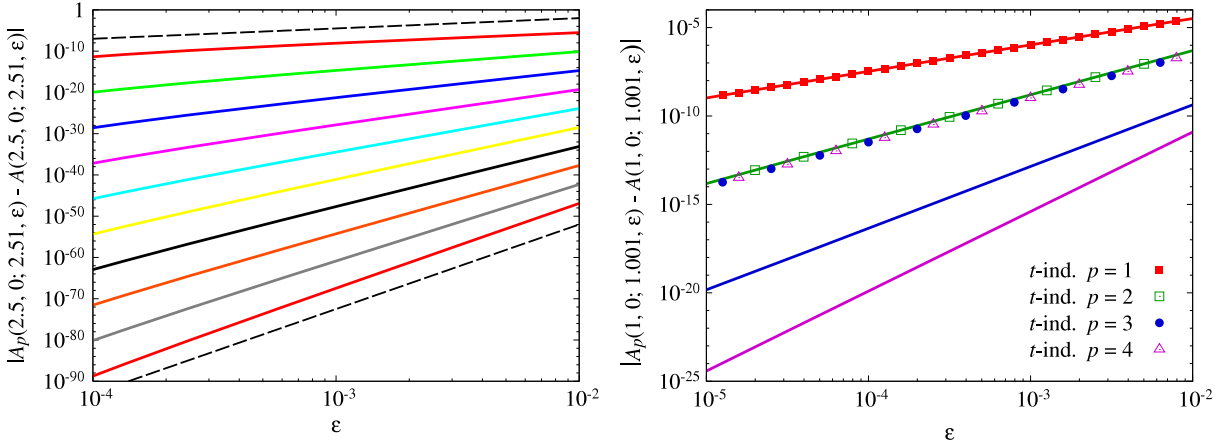


Figure 1. Deviations of amplitudes as functions of propagation time $\varepsilon = t_b - t_a$ for the harmonic oscillator (6.2) with $\omega = 1$, rescaled with the Grosche factor $\zeta(t) = \sqrt{t^2 + 1}$. (Left) Deviations of amplitudes $|A_p(2.5, 0; 2.51, \varepsilon) - A(2.5, 0; 2.51, \varepsilon)|$ as functions of ε , calculated analytically for $p = 2, 4, 6, 8, 10, 12, 14, 16, 18, 20$ from top to bottom. The dashed lines are proportional to $\varepsilon^{2.5}$ and $\varepsilon^{20.5}$ and demonstrate the perfect scaling of the corresponding level $p = 2$ and 20 results. (Right) Comparison of deviations $|A_p(1, 0; 1.001, \varepsilon) - A(1, 0; 1.001, \varepsilon)|$ calculated using the correct level $p = 1, 2, 3, 4$ effective potentials (full lines, top to bottom) with the deviations obtained for the same levels p of previously derived effective actions [48] for the case of time-independent potential. Deviations for different levels p of time-independent effective actions correspond to different point types.

programming language. In order to be able to resolve decreasingly small errors associated with higher levels p of the effective potential, we decided to consider at first some exactly solvable potentials.

In [67] it was shown that a generalized Duru–Kleinert transformation [21, 68, 69] allows one to map the transition amplitude for a time-independent potential $V(x)$ to the corresponding transition amplitude for the time-dependent potential

$$V_G(x, t) = \frac{1}{\zeta^2(t)} V\left(\frac{x}{\zeta(t)}\right), \quad (6.1)$$

where $\zeta^2(t) = \zeta_0 + \zeta_1 t + \zeta_2 t^2$ is a general quadratic polynomial in time. Figure 1 presents the numerical results for the time-dependent harmonic oscillator potential, where the time dependence is introduced by using the Grosche rescaling factor $\zeta(t) = \sqrt{1 + t^2}$:

$$V_{G,HO}(x, t) = \frac{\omega^2 x^2}{2(1 + t^2)^2}. \quad (6.2)$$

In the left plot of figure 1 we see that the obtained discretized amplitudes converge to the continuum limit systematically faster and faster when we use higher-level effective actions. This log–log plot demonstrates that the analytically derived law $\varepsilon^{p+1/2}$ for deviations of single-particle discretized transition amplitudes in $d = 1$ from the continuum transition amplitudes holds perfectly, which verifies numerically our analytical results. The deviations are calculated using the analytically known continuous transition

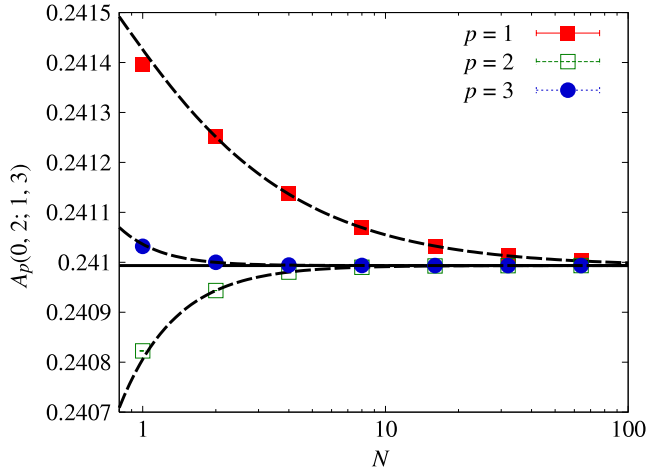


Figure 2. Convergence of numerical Monte Carlo results for the transition amplitude $A_p(0, 2; 1, 3)$ as a function of the number of time steps N for the time-dependent harmonic oscillator (6.2) with $\omega = 1$, calculated with level $p = 1, 2, 3$ effective actions. The dashed lines give the fitted functions $A_p + B_p/N^p + \dots$, where the constant term A_p corresponds to the continuum-theory amplitude $A_p(0, 2; 1, 3)$. The number of MC samples was $N_{\text{MC}} = 2 \times 10^9$. MC error bars of around 2×10^{-8} for all values of p are shown on the graph.

amplitude [67]. The graph on the right of figure 1 illustrates the importance of terms with time derivatives of the potential in higher-order effective actions. In this plot we show deviations of discretized transition amplitudes calculated using the effective actions for time-independent potentials, derived in [48], and compare them with the deviations of discretized transition amplitudes calculated with the correct effective actions, derived here for the case of time-dependent potentials. As can be seen from the graph, time-independent effective actions do not improve results after level $p = 2$, due to the fact that terms containing time derivatives of the potential are not systematically eliminated from deviations when such effective actions are used. If we use expressions derived for time-dependent potentials, as expected, the deviations are systematically reduced when we increase level p .

To show that the derived short-time effective actions can be used for calculating long-time transition amplitudes using the standard time-discretization approach for path integrals, we display in figure 2 the convergence of the discretized long-time transition amplitude for the Grosche-rescaled harmonic oscillator as a function of the number of time steps N . As expected, we have obtained $1/N^p$ behavior, in accordance with our earlier conclusion on the N -scaling of errors in this case. The numerical results presented in this graph are obtained using the Monte Carlo SPEEDUP [65] code, which was modified to include time-dependent effective actions implemented to high orders in the C programming language.

The second exactly solvable model that we have considered is the forced harmonic oscillator [61],

$$V_{\text{FHO}}(x, t) = \frac{1}{2}\omega^2 x^2 - x \sin \Omega t, \quad (6.3)$$

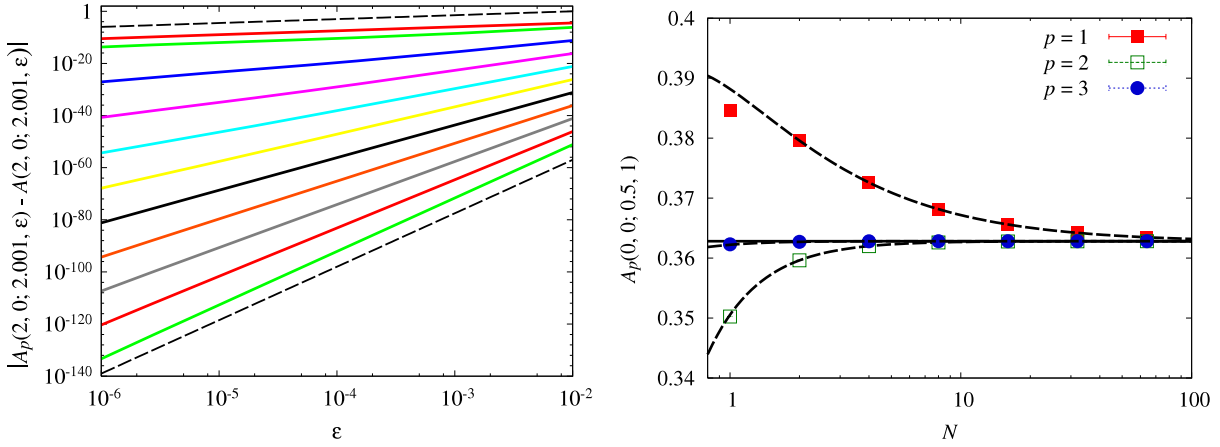


Figure 3. (Left) Deviations $|A_p(2, 0; 2.001, \varepsilon) - A(2, 0; 2.001, \varepsilon)|$ as a function of propagation time ε for the forced harmonic oscillator (6.3) with $\omega = \Omega = 1$, calculated analytically for $p = 1, 2, 4, 6, 8, 10, 12, 14, 16, 18, 20$ from top to bottom. The dashed lines are proportional to $\varepsilon^{1.5}$ and $\varepsilon^{20.5}$, and demonstrate the perfect scaling of the corresponding level $p = 1$ and 20 results. (Right) Convergence of numerical Monte Carlo results for the transition amplitude $A_p(0, 0; 0.5, 1)$ as a function of the number of time steps N for $p = 1, 2, 3$. As before, dashed lines give the fitted functions $A_p + B_p/N^p + \dots$, demonstrating the expected $1/N^p$ scaling of the deviations. The number of MC samples was $N_{\text{MC}} = 2 \times 10^9$. MC error bars of around 8×10^{-7} for all values of p are shown in the graph.

where Ω denotes the frequency of the external driving field. Figure 3 presents numerical results for this model for $\omega = \Omega = 1$. The top plot gives deviations for the case of short-time transition amplitude, calculated analytically using level p effective action. We see again a perfect ε -scaling of deviations. The bottom plot shows convergence of a long-time transition amplitude as a function of the number of time steps N , illustrating the expected $1/N^p$ behavior.

We have numerically also considered the non-trivial case of a pure quartic oscillator $V_{\text{PQ}}(x) = gx^4/24$ rescaled with the same Grosche factor $\zeta(t) = \sqrt{1+t^2}$:

$$V_{\text{G,PQ}}(x, t) = \frac{gx^4}{24(1+t^2)^3}. \quad (6.4)$$

This model is not exactly solvable, but the continuous transition amplitude can be determined numerically. To this end one could use the Grosche mapping, while relying on the previous numerical approach [48], providing exact transition amplitudes for the time-independent counterpart of the potential V_{PQ} . Another possibility is based on numerically obtained results from the modified SPEEDUP code, relying on the fitting of discretized amplitudes to the $\varepsilon \rightarrow 0$ limit. As we can see from figure 4, the numerical results exhibit a perfect scaling behavior for this non-trivial model as well. The power-law scaling of deviations in the calculated discretized transition amplitudes up to exceedingly small values fully verifies the analytic derivation of effective actions that has been presented.

As we have demonstrated during our analysis of several examples, the main advantage of the effective action approach is the calculation of transition amplitudes with high

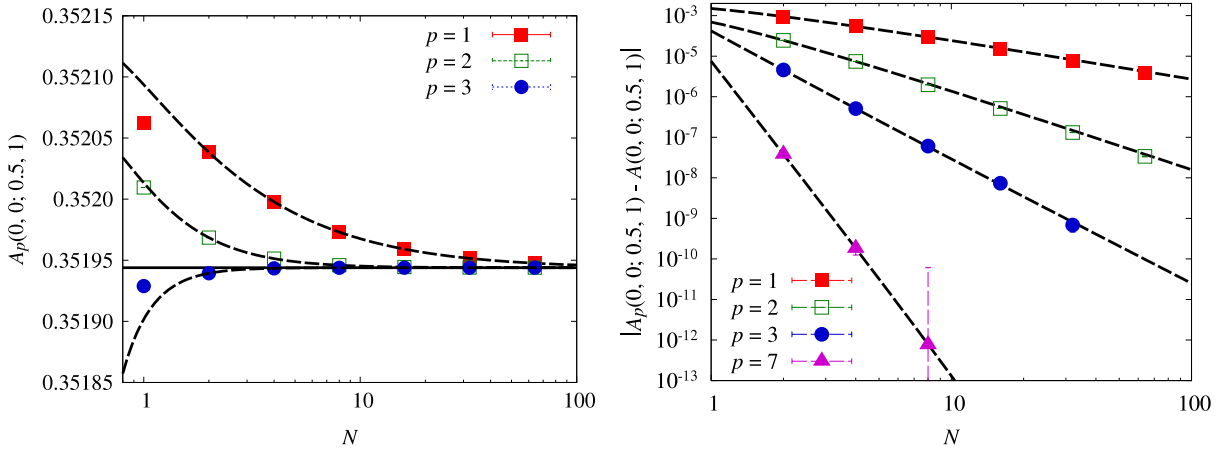


Figure 4. (Left) Convergence of numerical Monte Carlo results for the transition amplitude $A_p(0, 0; 0.5, 1)$ as a function of the number of time steps N for the pure quartic oscillator (6.4) with the anharmonicity $g = 0.1$, rescaled by the Grosche factor $\zeta(t) = \sqrt{t^2 + 1}$, and calculated with level $p = 1, 2, 3$ effective actions. As before, dashed lines give the fitted functions $A_p + B_p/N^p + \dots$. (Right) In order to convincingly demonstrate the expected dominant $1/N^p$ behavior of deviations, we plot $|A_p(0, 0; 0.5, 1) - A(0, 0; 0.5, 1)|$ as a function of the number of time steps N for $p = 1, 2, 3, 7$. The dashed lines are fitted polynomials $A_p + B_p/N^p + \dots$, the same as on the top graph. The exact value of the amplitude is obtained as the constant term from fitting $p = 7$ results. The number of Monte Carlo samples was $N_{\text{MC}} = 1.6 \times 10^{13}$ for $p = 7$, in order to be able to resolve the exceedingly small deviations from the exact value of the amplitude. For $p = 1, 2, 3$ we used much smaller values of N_{MC} , typically 10^8 – 10^{10} . MC error bars of around 2×10^{-10} for $p = 1, 2, 3$ and 6×10^{-11} for $p = 7$ are shown in both graphs.

precision, which can be improved by using higher levels p . In practical applications, this increase in the precision is counterweighted by having to evaluate increasingly complex expressions for the effective action. Figure 5 gives the comparison of the increase in the computational complexity of numerical codes for different levels p for the three models considered. As we can see, depending on the model, CPU time increases 5–10 times for $p = 7$, and clearly the benefit of seven orders of magnitude increase in the precision of calculations far outweighs the CPU time increase. However, as p increases, the computational complexity will become too high. Since this strongly depends on the model, one has to perform a small-scale complexity study, similar to the one presented in figure 5, in order to find the optimal value of level p to be used in numerical simulations.

While the presented approach is excellently suited for applications where high-precision transition amplitudes are necessary, e.g. the calculation of partition functions, other higher-order schemes may be preferred for solving different types of problems. For example, the split operator method [28, 34], [36]–[38], [58] is ideally suited for studying both the real- and the imaginary-time evolution of various quantum systems. Furthermore, it has the advantage that it can be implemented in any chosen representation, which is appropriate for the quantum system, while the effective action approach relies on using the coordinate representation.

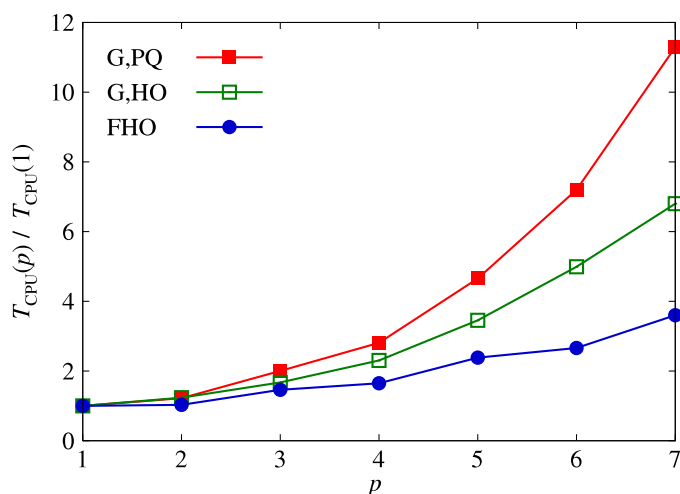


Figure 5. Increase in the computational complexity of numerical simulations as a function of level p for the three models considered (Grosche-rescaled harmonic oscillator—G, HO; forced harmonic oscillator—FHO; Grosche-rescaled pure quartic oscillator—G, PQ). The complexity is measured by the relative increase in the CPU time $T_{\text{CPU}}(p)/T_{\text{CPU}}(1)$ for calculation of transition amplitudes from figures 2 to 4, for each model correspondingly. The number of Monte Carlo samples was $N_{\text{MC}} = 2 \times 10^9$ and number of time steps $N = 64$.

7. Conclusions

We have presented an analytic procedure for deriving the short-time expansion of the propagator for a general one-particle non-relativistic quantum system in a time-dependent potential up to previously inaccessible high orders. The procedure is based on recursively solving both the forward and backward Schrödinger equation for the transition amplitude. Following an earlier approach for time-independent potentials [48], we have derived recursion relations which allow an efficient analytic calculation of the effective potential to arbitrarily high orders in the propagation time ε in the imaginary time. The analytically derived results are numerically verified by studying several simple models.

The presented approach will be further expanded and generalized to many-body and multi-component systems in the forthcoming publication [1]. The next paper will also include generalization of the present imaginary-time approach to the real-time formalism, and its extensive numerical verification.

Acknowledgments

We thank Hagen Kleinert for several useful suggestions. This work was supported in part by the Ministry of Science and Technological Development of the Republic of Serbia, under project No. ON171017 and bilateral projects PI-BEC and NAD-BEC, funded jointly with the German Academic Exchange Service (DAAD). Numerical simulations were run on the AEGIS e-Infrastructure, supported in part by FP7 project EGI-InSPIRE, HP-SEE and PRACE-1IP.

References

- [1] Balaž A, Vidanović I, Bogojević A, Belić A and Pelster A, 2011 *J. Stat. Mech.* P03005
- [2] Bretin V, Stock S, Seurin Y and Dalibard J, 2004 *Phys. Rev. Lett.* **92** 050403
- [3] Fetter A L, Jackson B and Stringari S, 2005 *Phys. Rev. A* **71** 013605
- [4] Abdullaev F Kh, Shaari J S and Wahiddin M R B, 2005 *Phys. Lett. A* **345** 237
- [5] Kling S and Pelster A, 2007 *Phys. Rev. A* **76** 023609
- [6] Theodorakis S and Constantinou Y, 2007 *Phys. Lett. A* **364** 497
- [7] Alon O E, Streltsov A I and Cederbaum L S, 2007 *Phys. Lett. A* **362** 453
- [8] Kling S and Pelster A, 2009 *Laser Phys.* **19** 1072
- [9] Mason P and Berloff N G, 2009 *Phys. Rev. A* **79** 043620
- [10] Aftalion A, Blanc X and Dalibard J, 2005 *Phys. Rev. A* **71** 023611
- [11] Aftalion A, Blanc X and Lerner N, 2009 *Phys. Rev. A* **79** 011603(R)
- [12] Fallani L, De Sarlo L, Lye J E, Modugno M, Saers R, Fort C and Inguscio M, 2004 *Phys. Rev. Lett.* **93** 140406
- [13] Miller D E, Chin J K, Stan C A, Liu Y, Setiawan W, Sanner C and Ketterle W, 2007 *Phys. Rev. Lett.* **99** 070402
- [14] Mun J, Medley P, Campbell G K, Marcassa L G, Pritchard D E and Ketterle W, 2007 *Phys. Rev. Lett.* **99** 150604
- [15] Deumens E, Diz A, Longo R and Öhrn Y, 1994 *Rev. Mod. Phys.* **66** 917
- [16] Boness T, Bose S and Monteiro T S, 2006 *Phys. Rev. Lett.* **96** 187201
- [17] Eisler V and Peschel I, 2008 *Ann. Phys.* **17** 410
- [18] Bellomo B, LoFranco R, Maniscalco S and Compagno G, 2008 *Phys. Rev. A* **78** 060302(R)
- [19] Muruganandam P and Adhikari S K, 2009 *Comput. Phys. Commun.* **180** 1888
- [20] Heller E J, 1975 *J. Chem. Phys.* **62** 1544
- [21] Kleinert H, 2009 *Path Integrals in Quantum Mechanics, Statistics, Polymer Physics, and Financial Markets* 5th edn (Singapore: World Scientific)
- [22] Schollwöck U, 2005 *Rev. Mod. Phys.* **77** 259
- [23] Hallberg K, 2006 *Adv. Phys.* **55** 477
- [24] Runge E and Gross E K U, 1984 *Phys. Rev. Lett.* **52** 997
- [25] Onida G, Reining L and Rubio A, 2002 *Rev. Mod. Phys.* **74** 601
- [26] Pernal K, Gritsenko O and Baerends E J, 2007 *Phys. Rev. A* **75** 012506
- [27] Crank J and Nicolson P, 1996 *Adv. Comput. Math.* **6** 207
- [28] Chin S A and Krotscheck E, 2005 *Phys. Rev. E* **72** 036705
- [29] Hernández E R, Janecek S, Kaczmarek M and Krotscheck E, 2007 *Phys. Rev. B* **75** 075108
- [30] Ciftja O and Chin S A, 2003 *Phys. Rev. B* **68** 134510
- [31] Sakkos K, Casulleras J and Boronat J, 2009 *J. Chem. Phys.* **130** 204109
- [32] Bandrauk A D and Shen H, 1993 *J. Chem. Phys.* **99** 1185
- [33] Blanes S and Moan P C, 2000 *Phys. Lett. A* **265** 35
- [34] Chin S A and Chen C R, 2002 *J. Chem. Phys.* **117** 1409
- [35] Baye D, Goldstein G and Capel P, 2003 *Phys. Lett. A* **317** 337
- [36] Omelyan I P, Mryglod I M and Folk R, 2002 *Phys. Rev. E* **66** 026701
- [37] Omelyan I P, Mryglod I M and Folk R, 2003 *Comput. Phys. Commun.* **151** 272
- [38] Goldstein G and Baye D, 2004 *Phys. Rev. E* **70** 056703
- [39] Zillich R E, Mayrhofer J M and Chin S A, 2010 *J. Chem. Phys.* **132** 044103
- [40] Evertz H G, Lana G and Marcu M, 1993 *Phys. Rev. Lett.* **70** 875
- [41] Prokofev N V, Svistunov B V and Tupitsyn I S, 1998 *Sov. Phys. JETP* **87** 310
- [42] Syljuåsen O F and Sandvik A W, 2002 *Phys. Rev. E* **66** 046701
- [43] Beard B B and Wiese U-J, 1996 *Phys. Rev. Lett.* **77** 5130
- [44] Breuer H P and Petruccione F, 2002 *The Theory of Open Quantum Systems* (New York: Oxford University Press)
- [45] Bogojević A, Balaž A and Belić A, 2005 *Phys. Rev. Lett.* **94** 180403
- [46] Bogojević A, Balaž A and Belić A, 2005 *Phys. Rev. B* **72** 064302
- [47] Bogojević A, Vidanović I, Balaž A and Belić A, 2008 *Phys. Lett. A* **372** 3341
- [48] Balaž A, Bogojević A, Vidanović I and Pelster A, 2009 *Phys. Rev. E* **79** 036701
- [49] Stojiljković D, Bogojević A and Balaž A, 2006 *Phys. Lett. A* **360** 205
- [50] Vidanović I, Bogojević A and Belić A, 2009 *Phys. Rev. E* **80** 066705
- [51] Vidanović I, Bogojević A, Balaž A and Belić A, 2009 *Phys. Rev. E* **80** 066706

- [52] Balaž A, Vidanović I, Bogojević A and Pelster A, 2010 *Phys. Lett. A* **374** 1539
- [53] Mak C H and Egger R, 1999 *J. Chem. Phys.* **110** 12
- [54] Symanzik K, 1982 *Mathematical Problems in Theoretical Physics: Conf. Berlin 1981 (Lecture Notes in Physics* vol 153) ed R Schrader *et al* (Berlin: Springer)
- [55] Fliegner D, Schmidt M G and Schubert C, 1994 *Z. Phys. C* **64** 111
- [56] Sheng Q, 1989 *IMA J. Numer. Anal.* **9** 199
- [57] Suzuki M, 1991 *J. Math. Phys.* **32** 400
- [58] Chin S A, Janecek S and Krotscheck E, 2009 *Comput. Phys. Commun.* **180** 1700
- [59] Bogojević A, Balaž A and Belić A, 2005 *Phys. Rev. E* **72** 036128
- [60] Feynman R P, 1948 *Rev. Mod. Phys.* **20** 367
- [61] Feynman R P and Hibbs A R, 1965 *Quantum Mechanics and Path Integrals* (New York: McGraw-Hill)
- [62] Feynman R P, 1972 *Statistical Mechanics* (New York: Benjamin)
- [63] Ceperley D M, 1995 *Rev. Mod. Phys.* **67** 279
- [64] Bogojević A, Balaž A and Belić A, 2005 *Phys. Lett. A* **344** 84
- [65] SPEEDUP C language and Mathematica code <http://www.scl.rs/speedup/>
- [66] Mathematica software package <http://www.wolfram.com/mathematica/>
- [67] Grosche C, 1993 *Phys. Lett. A* **182** 28
- [68] Storchak S N, 1989 *Phys. Lett. A* **135** 77
- [69] Pelster A and Wunderlin A, 1992 *Z. Phys. B* **89** 373